Inflammation, Vol. 42, No. 2, April 2019 (© 2018)
DOI: 10.1007/s10753-018-0909-1

ORIGINAL ARTICLE

Role of Thymoquinone in Cardiac Damage Caused by Sepsis from BALB/c Mice

Hongyang Liu,[1] Yan Sun,[2] Ying Zhang,[3] Guang Yang,[1] Lipeng Guo,[4] Yue Zhao,[5] and Zuowei Pei[6,7]

Abstract— Sepsis is a major health complication causing patient mortality and increased healthcare costs. Cardiac dysfunction, an important consequence of sepsis, affects mortality. We previously reported that thymoquinone (TQ) protected against hyperlipidemia and doxorubicin-induced cardiac damage. This study investigated the possible protective effects of TQ against cardiac damage in septic BALB/c mice. Eight-week-old male BALB/c mice were divided into four groups: control, TQ, cecal ligation and puncture (CLP), and TQ + CLP. CLP was performed after 2-week TQ gavage. After 48 h, we measured the histopathological alterations of the cardiac tissue and the plasma levels of troponin-T (cTnT) and ATP. We evaluated autophagy (p62 and beclin 1), pyroptosis (NLRP3, caspase-1, interleukin [IL]-1β, and IL-18) at the gene and protein levels and IL-6 and tumor necrosis factor-α (TNF-α) at the gene level. Our results demonstrated that TQ administration significantly reduced intestinal histological alterations. TQ inhibited plasma cTnT levels; improved ATP; significantly inhibited p62, NLRP3, caspase-1, IL-1β, IL-18, IL-6, TNF-α, and MCP-1expressions; and increased beclin 1 and IL-10 level. The phosphatidylinositide 3-kinase level was significantly decreased in the TQ + CLP group versus the CLP group. These results suggest that TQ effectively modulates autophagy, pyroptosis, and pro-inflammatory, making it important in the treatment of sepsis-induced cardiac damage.

KEY WORDS: sepsis; thymoquinone; cardiac damage; pyroptosis; BALB/c mice.

INTRODUCTION

Sepsis is defined as a life-threatening pathological alteration to the severe condition of patients hospitalized in intensive care units. Over the past few decades, researches have noted a significant increase in the morbidity of sepsis [1–3]. Although increasing evidence suggests that the enhanced production of many inflammatory cytokines can directly or indirectly cause cardiac damage, the precise mechanisms of myocardial dysfunction in sepsis remain undefined [4–6]. In recent years, many studies have shown that autophagy is a tightly regulated intracellular catabolic process that serves as the cellular quality control mechanism of the disposal of damaged and dysfunctional

Hongyang Liu and Yan Sun contributed equally to this work.

[1] Department of Heart Intensive Care Unit, The First Affiliated Hospital of Dalian Medical University, No.193 Lianhe Road, Dalian, China
[2] Department of Cardiology, Zhejiang Rongjun Hospital, No.309 Shuangyuan Road, Jiaxing, Zhejiang, China
[3] Department of Cardiology, The First Affiliated Hospital of Dalian Medical University, 193# Lianhe Road, Dalian, China
[4] Department of Cardiology, Dalian Third People's Hospital Affiliated to Dalian Medical University, No.40 Qianshan Road, Dalian, China
[5] Graduate school of Dalian Medical University, No.9 Lvshun South Road, Dalian, China
[6] Department of Cardiology, Affiliated Zhongshan Hospital of Dalian University, No. 6 Jiefang Street, Dalian, 116001, China
[7] To whom correspondence should be addressed at Department of Cardiology, Affiliated Zhongshan Hospital of Dalian University, No. 6 Jiefang Street, Dalian, 116001, China. E-mail: pzw_dl@163.com

organelles and protein aggregates; thus, it is widely implicated in pathophysiological processes, including cardiovascular diseases [7, 8]. Pyroptosis is an inflammatory form of programmed cell death. In general, pyroptosis protects multicellular host organisms against invasive pathogenic bacteria and microbial infections; however, it also causes sepsis and septic shock when overactivated [9–12]. To date, however, available treatments to protect against sepsis-induced cardiac damage have been varied and limited.

Interest has recently grown in the use of natural phytochemical compounds for the alternative treatment of several conditions including cardiovascular diseases. One of these compounds, thymoquinone (TQ), is the main active ingredient of *Nigella sativa*, commonly known as black cumin or black seed, an annual flowering plant native to Mediterranean countries [13]. We previously reported that TQ protected against hyperlipidemia and doxorubicin-induced cardiac damage [14, 15].

Here, we investigated the role of TQ in sepsis-induced cardiac damage. Our results contribute to our understanding of the beneficial role and mechanism of action of TQ in sepsis-induced cardiac disorders. This study reveals a novel role of TQ in modulating autophagy, pyroptosis, and inflammatory expression and provides a new potential application of treating sepsis-induced cardiac damage.

Animals

All animal studies were approved by the Animal Studies Committee of the affiliated Zhongshan Hospital of Dalian University. Male BALB/c mice were purchased from Beijing Vital River Lab Animal Technology Co., Ltd. (Beijing, China) and maintained under controlled conditions (temperature, 23–25 °C; humidity, 40–60%; 12-h light/dark cycle).

Murine Model of Sepsis

To induce polymicrobial sepsis, we used an established murine model of cecal ligation and puncture (CLP) as previously described [16]. Briefly, the mice were anesthetized with sodium pentobarbital (100 mg/kg intraperitoneal). The peritoneum was opened and the bowel was exposed. Two-thirds of the caecum was tied off and punctured once with a 21-gauge needle. Gentle pressure was applied at the perforation sites to extrude a small amount of feces, which was then returned to the peritoneal cavity. The laparotomy site was then stitched. Sham-operated mice underwent the same procedure, which included opening the peritoneum and exposing the bowel but did not include the ligation or needle perforation. The 48 eight-week-old male mice were randomly divided into four groups ($n = 12$ each): control; TQ (50 mg/kg/day; Sigma-Aldrich, St. Louis, MO, USA), CLP, and CLP + TQ. CLP was performed after the mice were subjected to 2-week TQ gavage. Forty-eight hours later, all surviving mice were killed and blood samples were obtained from the inferior vena cava, collected in serum tubes, and stored at − 80 °C until being used. Coronal sections of the cardiac tissues were fixed in 10% formalin and then embedded in paraffin for histological evaluation. The remainder of the cardiac tissues was snap-frozen in liquid nitrogen for mRNA or immunoblotting analysis. All animal experiments were performed in accordance with the Guide for the Care and Use of Laboratory Animals. The study was approved by the ethical committee of the affiliated Zhongshan Hospital of Dalian University.

Serum Analysis

Serum concentrations of cTnT and ATP were measured using an enzyme-linked immunosorbent assay kit (Westang, Shanghai, China).

Hematoxylin and Eosin Staining

Cardiac tissues were fixed in 10% buffered formalin solution, followed by paraffin embedding. Serial sections (4 μm) were subjected to hematoxylin and eosin staining for assessing the pathological changes.

Morphologic Analysis and immunohistochemistry Immunohistochemistry was performed using a Histone Simple Stain Kit (Nichirei, Tokyo, Japan) according to the manufacturer's instructions. Briefly, paraffin-embedded sections were deparaffinized with xylene and then rehydrated in a descending series of ethanol washes. The sections were treated for 15 min with 3% H_2O_2 in methanol to inactivate endogenous peroxidases and then incubated at room temperature for 1 h with primary antibodies to p62 (rabbit anti-p62 antibody, 1:200; Proteintech, Wuhan, China), beclin 1 (rabbit anti-beclin 1 antibody, 1:200; Proteintech), caspase-1 (rabbit anti-caspase-1 antibody, 1:200; Proteintech), NLRP3 (rabbit anti-NLRP3 antibody, 1:200; Proteintech), interleukin (IL)-1β (rabbit anti- IL-1β antibody, 1:500; Proteintech), and IL-18 (rabbit anti-IL-18 antibody, 1:400; Proteintech). Tissue sections were observed under microscopy (Olympus, Tokyo, Japan).

RNA Isolation and Real-Time Reverse Transcription Polymerase Chain Reaction

Total RNA was isolated from cardiac tissues using ISOGEN (Nippon Gene, Tokyo, Japan) according to the manufacturer's protocol. Complementary DNA (cDNA) was synthesized from the total RNA using a first-strand cDNA synthesis kit (SuperScript VILO cDNA Synthesis Kit; Life Technologies Carlsbad, CA, USA) according to the manufacturer's protocol. Gene expression was quantitatively analyzed by real-time reverse transcription polymerase chain reaction using fluorescent SYBR Green technology (Light Cycler; Roche Molecular Biochemicals). Beta-actin cDNA was amplified and quantitated in each cDNA preparation to normalize the relative amounts of the target genes. Primer sequences are listed in Table 1.

Western Blotting for Cardiac Tissues

Proteins were extracted from cardiac tissues using radioimmunoprecipitation assay buffer (P0013B; Beyotime, Shanghai, China). Samples were electrophoresed on 10% sodium dodecyl sulphate–polyacrylamide gel electrophoresis and proteins were transferred to polyvinylidene fluoride membranes (Immobilon, Millipore, Billerica, MA, USA). The membranes were blocked in Tris-buffered saline with 0.1% Tween-20 containing 5% skim milk and then incubated in primary antibody diluent (P0023A; Beyotime) and gently shaken overnight at 4 °C. Primary antibodies against p62 (rabbit anti-p62 antibody, 1:1000; Proteintech), beclin 1 (rabbit anti-beclin 1 antibody, 1:1000; Proteintech), caspase-1 (rabbit anti-caspase-1 antibody, 1:100; Proteintech), NLRP3 (rabbit anti-NLRP3 antibody, 1:1000; Proteintech), IL-1β (rabbit anti-IL-1 β antibody, 1:1000; Proteintech), IL-18 (rabbit anti-IL-18 antibody, 1:1000; Proteintech), and anti-β-actin (1:1000; Cell Signaling Technology). Membranes were then incubated with secondary antibody (anti-rabbit Ig-G, 1:1000; Cell Signaling Technology) for 1 h. This analysis was performed independently three times. Protein levels are expressed as protein/β-actin ratios to minimize loading differences. The relative signal intensity was quantified using NIH Image J software.

Statistical Analysis

All data are presented as mean ± SEM. The statistical analysis was performed using SPSS version 23.0 (SPSS Inc., Chicago, IL, USA). Inter-group variation was measured by one-way analysis of variance and a subsequent Tukey's test. The minimal level for significance was $P < 0.05$.

RESULTS

Metabolic Characterization

The metabolic characteristics of the BALB/c mice in the four groups after treatment are summarized in Fig. 1.

Table 1. Primer oligonucleotide sequences

Gene	Primers
TNF-α	F:5′-TCTCATGCACCACCATCAAGGACT-3′ R:5′-ACCACTCTCCCTTTGCAGAACTCA-3′
IL-6	F:5′-TACCAGTTGCCTTCTTGGGACTGA-3′ R:5′-TAAGCCTCCGACTTGTGAAGTGGT-3′
MCP-1	F:5′-ACTGAAGCCAGCTCTCTCTTCCTC-3′ R:5′-TTCCTTCTTGGGTCAGCACAGAC-3′
IL-10	F:5′-GACAACATACTGCTAACCGACT-3′ R:5′-ATCACTCTTCACCTGCTCCAC-3′
NLRP3	F:5′-CTGCGGACTGTCCCATCAAT-3′ R:5′-AGGTTGCAGAGCAGGTGCTT-3′
IL-1β	F: 5′-TGCCACCTTTTGACAGTGAT-3′ R: 5′-TGTGCTGCTGCGAGATTTGA-3′
IL-18	F: 5′-ATGGCTGCTGAACCAGTAGAAG-3′ R: 5′-CAGCCATACCTCTAGGCTGGC-3′
Caspase-1	F: 5′-AACCAGGAGAATGTTTCCAACCT-3′ R: 5′-AAACACCAGGCCAAGCTTCTT-3′
β-actin	F:5′-CGATGCCCTGAGGGTCTTT-3′ R:5′-TGGATGCCACAGGATTCCAT-3′

TNF-α tumor necrosis factor-α, *IL-6* interleukin-6, *IL-1β* interleukin-1β

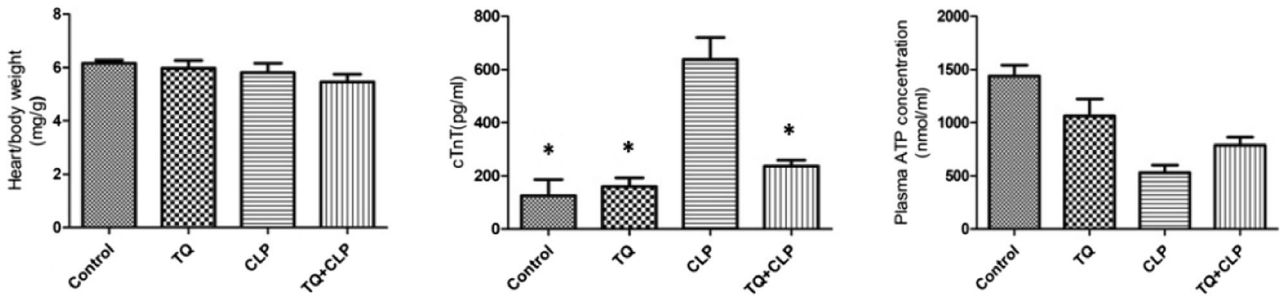

Fig. 1. Metabolic data from the BALB/c mice of the four groups after treatment. Heart/body weights as well as cTnT and ATP expressions of the four groups after treatment are presented. Data are mean ± SEM; $n = 10–12$ per group. *$P < 0.05$ *vs* CLP group.

Heart/body weights did not differ among the four groups. The levels of cTnT were markedly increased in the CLP group but significantly decreased in the TQ + CLP group. There were no differences among the control, TQ and TQ + CLP groups.

TQ Reduced Cardiac Histopathological Damage in CLP Group Mice

To evaluate inflammatory cell infiltration into the cardiac tissue, hematoxylin and eosin staining was performed (Fig. 2). The TQ + CLP group mice showed markedly reduced inflammatory cell infiltration in the cardiac tissue compared to CLP group mice. These results indicate that TQ reduced leukocyte infiltration into the cardiac tissue in BALB/c mice.

TQ Decreased p62 and Increased Beclin 1 Expression in the Cardiac Tissues of CLP Group Mice

To evaluate p62 and beclin 1 expression in the cardiac tissues, p62 and beclin 1 immunostainings were performed (Fig. 3a). The TQ + CLP group had markedly reduced p62 and increased beclin 1 expressions in the cardiac tissues compared to the CLP group. Immunoblotting was performed for p62 and beclin 1 proteins (Fig. 3b). We found that p62 protein expression was decreased and beclin 1 protein expression was significantly increased in the TQ + CLP group compared with the CLP group (Fig. 3c). These results indicate that TQ reduced p62 and increased beclin 1 expressions in the CLP group mice.

TQ Reduced Pyroptosis Expression in the Cardiac Tissue of CLP Group Mice

To evaluate pyroptosis expression in the cardiac tissues, NLRP3, caspase-1, IL-1β, and IL-18 immunohistochemical analysis was performed (Fig. 4b). We found the TQ + CLP group had markedly reduced NLRP3, caspase-1, IL-1β, and IL-18 expression in cardiac tissues compared to the CLP group. Reverse transcription polymerase chain reaction was performed for NLRP3, caspase-1, IL-1β, and IL-18 gene expression (Fig. 4a). We found that NLRP3, caspase-1, IL-1β, and IL-18 gene expressions were significantly suppressed in the TQ + CLP group compared to the CLP group. Immunoblotting was performed for NLRP3, caspase-1, IL-1β, and IL-18 proteins (Fig. 4c). We found that NLRP3, caspase-1, IL-1β, and IL-18 expressions were significantly suppressed in the TQ + CLP group compared to the CLP group (Fig. 4d). These results indicated that TQ reduced NLRP3, caspase-1, IL-1β, and IL-18 expression in the CLP group mice.

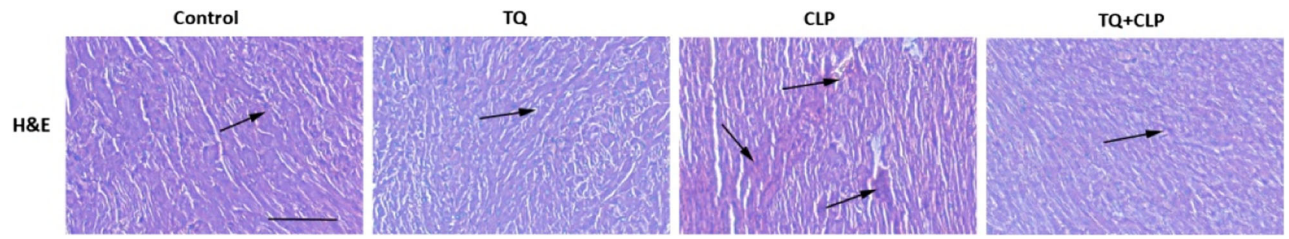

Fig. 2. Inflammatory cell infiltration in the cardiac tissue from the BALB/c mice of the four groups after treatment. Representative hematoxylin and eosin staining for morphology damage in the cardiac tissue of mice with different diets. Scale bar = 100 μm. The arrows indicate damage.

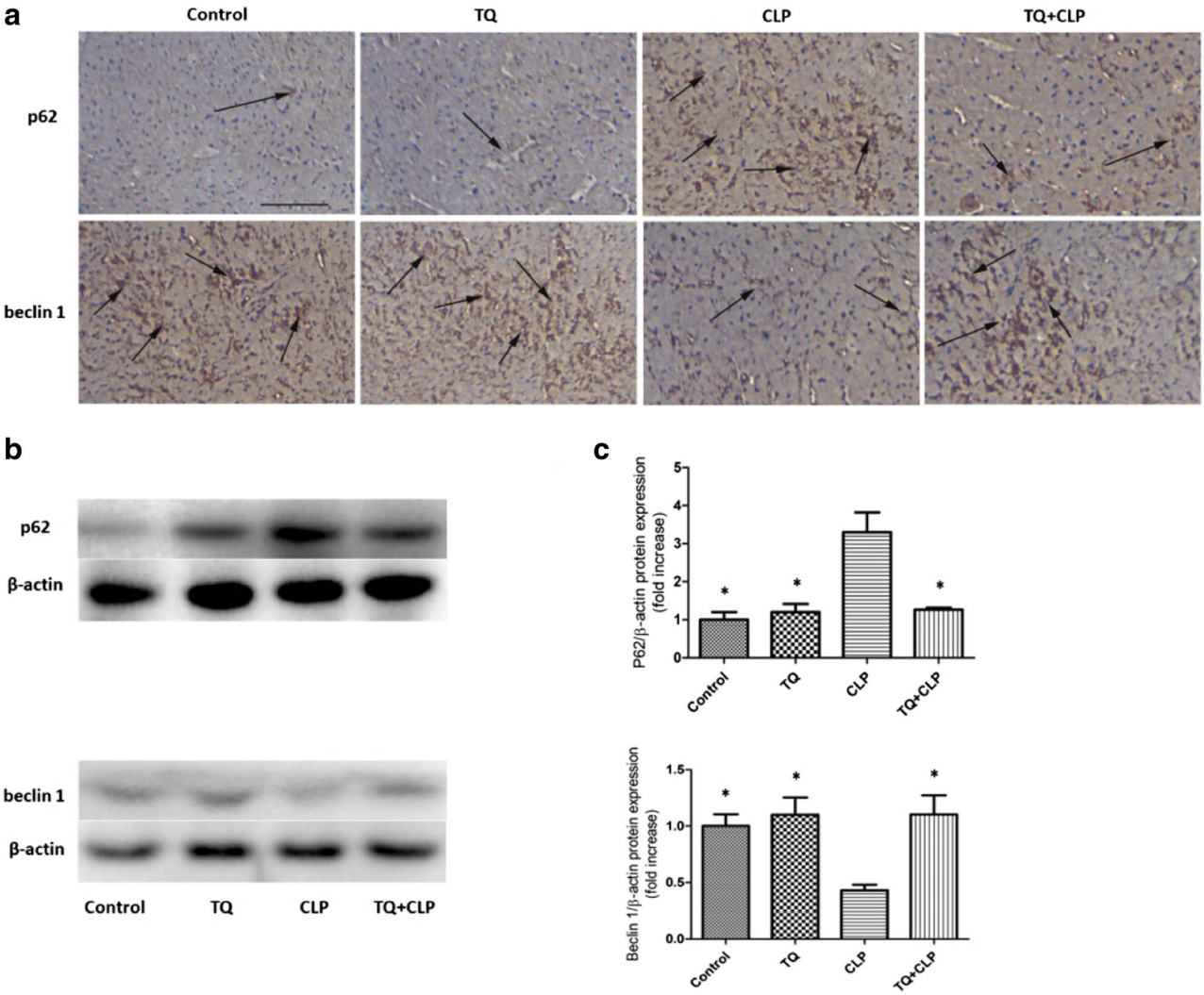

Fig. 3. P62 and beclin 1 expression in the cardiac tissues from the BALB/c mice of the four groups after treatment. **a** Representative immunohistochemistry of p62 and beclin 1 in cardiac tissues. Scale bar = 100 μm. Arrows indicate positively stained cells. **b** Immunoblotting for p62 and beclin 1 in cardiac tissues. **c** Bar graph showing quantification of p62 and beclin 1 protein expressions. Data are given as mean ± SEM; $n = 3–4$ in each group. $^*P < 0.05$ *vs.* CLP group.

TQ Reduced Phosphatidylinositide 3-Kinase Expression in Cardiac Tissues of CLP Group Mice

To investigate the effect of TQ on regulation of the phosphatidylinositide 3-kinase (PI3K) signaling pathway, we analyzed the PI3K level in the respective treatment groups by performing immunoblotting (Fig. 5a). We found a higher PI3K expression level in the CLP group than in the control group. Additionally, the TQ + CLP group exhibited significantly suppressed PI3K levels compared the CLP group (Fig. 5b).

TQ Reduced Pro-inflammatory Cytokines (IL-6, TNF-α, and MCP-1) Gene and Increased IL-10 Gene Expression in Cardiac Tissues of CLP Group Mice

To examine the involvement of pro-inflammatory cytokines in the gene expression of cardiac tissues of the four groups of mice, the gene expressions of IL-6, TNF-α, MCP-1, and IL-10 were measured using real-time polymerase chain reaction (Fig. Fig. 6). IL-6, TNF-α, and MCP-1 expressions were upregulated in the CLP group; however, this upregulation was attenuated in the TQ + CLP

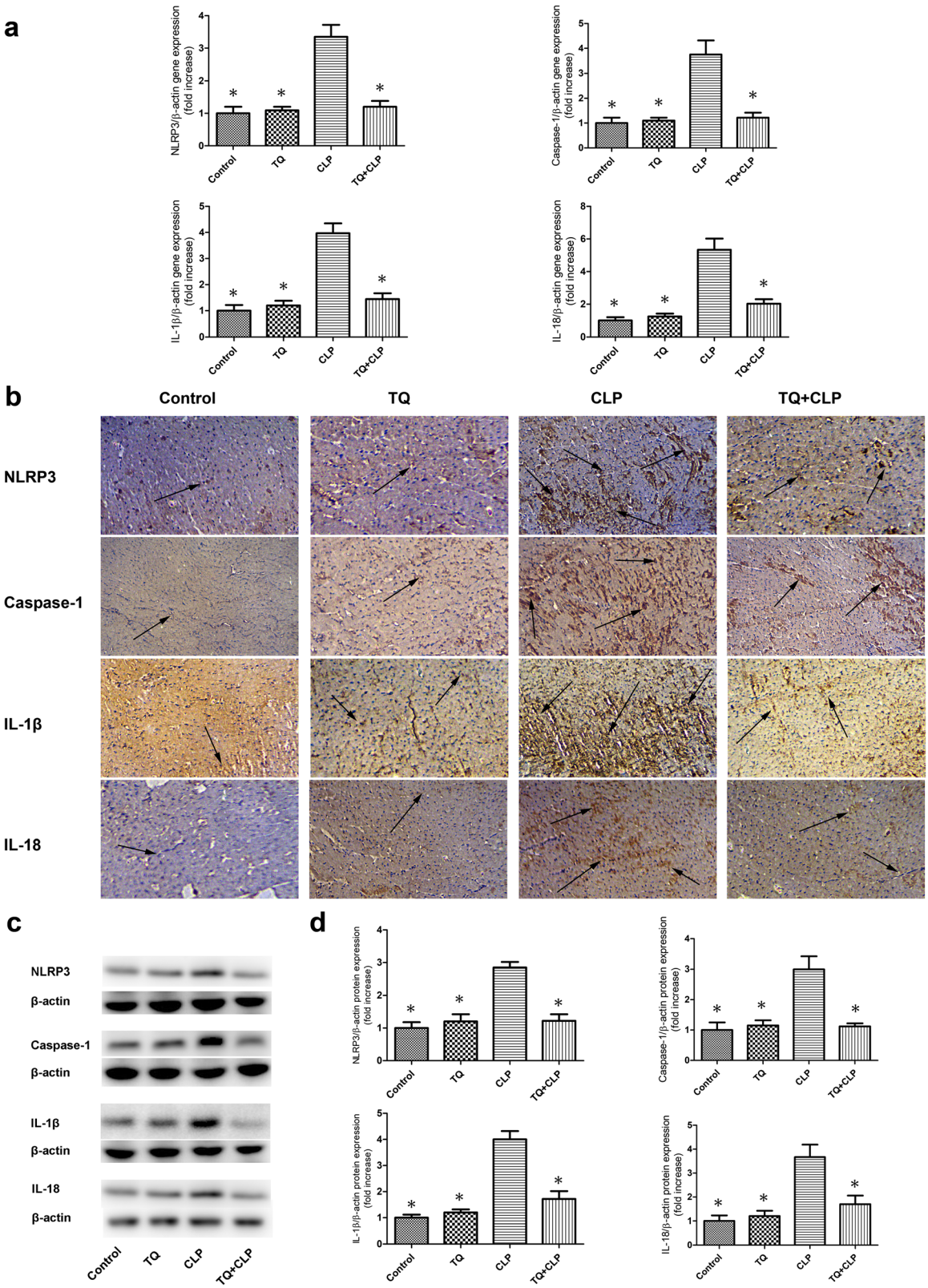
a
NLRP3/β-actin gene expression (fold increase)
Caspase-1/β-actin gene expression (fold increase)
IL-1β/β-actin gene expression (fold increase)
IL-18/β-actin gene expression (fold increase)
Control
TQ
CLP
TQ+CLP
b
Control
TQ
CLP
TQ+CLP
NLRP3
Caspase-1
IL-1β
IL-18
c
NLRP3
β-actin
Caspase-1
β-actin
IL-1β
β-actin
IL-18
β-actin
Control
TQ
CLP
TQ+CLP
d
NLRP3/β-actin protein expression (fold increase)
Caspase-1/β-actin protein expression (fold increase)
IL-1β/β-actin protein expression (fold increase)
IL-18/β-actin protein expression (fold increase)
Control
TQ
CLP
TQ+CLP

Fig. 4. NLRP3, caspase-1, IL-1β, and IL-18 expressions in the cardiac tissues from the BALB/c mice of the four groups after treatment. **a** Relative mRNA expression of NLRP3, caspase-1, IL-1β, and IL-18 in the cardiac tissue. **b** Representative immunohistochemistry of NLRP3, caspase-1, IL-1β, and IL-18 in cardiac tissues. Scale bar = 100 μm. The arrows indicate positively stained cells. **c** Immunoblotting for NLRP3, caspase-1, IL-1β, and IL-18 in the cardiac tissues. **d** Bar graph showing quantification of NLRP3, caspase-1, IL-1β, and IL-18 protein expressions. Data are given as mean ± SEM; $n = 3–4$ in each group. *$P < 0.05$ *vs.* the CLP group.

group. IL-10 expressions were downregulated in the CLP group; however, this downregulation was increased in the TQ + CLP group.

DISCUSSION

This study demonstrated that TQ has a protective effect against cardiac damage *via* autophagy, pyroptosis, and pro-inflammatory cytokine expression. According to these metabolic characteristics, we found that cTnT increased in the CLP group compared with the control group. In sepsis, cTnT is an important indicator of cardiac damage. These results are in agreement with the report by Ming Chu [17]. Interestingly, cTnT was significantly suppressed in the TQ + CLP group compared to that in the CLP group. However, further studies are needed to clarify the mechanisms. It is generally accepted that inflammatory mediators activate numerous molecular signals to produce cardiosuppressive cytokines, resulting in septic cardiomyopathy [18]. As a result, increased inflammatory cell infiltration led to the release of greater inflammation in the CLP group than the TQ + CLP group. Taken together, the serum and histological results confirmed cardiac damage in the CLP group; however, the damage was significantly suppressed in the TQ + CLP group.

Recent studies reported that autophagy also plays an important role in septic myocardial depression. Accumulating evidence has shown that autophagic activity in cardiomyocytes changes during sepsis, but the results are unclear [19, 20]. P62 and beclin 1 are two major proteins in autophagy, and previous studies showed that p62 expression increased and beclin 1 expression decreased in cardiac damage and in sepsis [21–23]. We obtained the same result in our study, in which we analyzed p62 and beclin 1 expression in the cardiac tissue with immunohistochemistry and immunoblotting and showed that p62 significantly increased and beclin 1 significantly decreased in the CLP group, whereas p62 markedly decreased and beclin 1 markedly increased in the TQ + CLP group compared with the CLP group.

Recent studies have reported that pyroptosis contributes to development of sepsis and septic shock [24, 25]. Pyroptosis induces an extensive inflammatory response [26, 27]. The role of the NLRP3 inflammasome has been established in various immune and inflammatory diseases [28, 29]. Wu and colleagues established a classic septic model in rats by CLP and studied the role of NLRP3 in sepsis by injecting rats with Nlrp3 short hairpin RNA plasmids (Nlrp3 shRNA). They found that Nlrp3 knockdown attenuated hyperbileacidaemia by restoring the abundance of hepatocyte transporters and suppressing the production of hepatic cytokines, neutrophil infiltration, and macrophage pyroptosis during

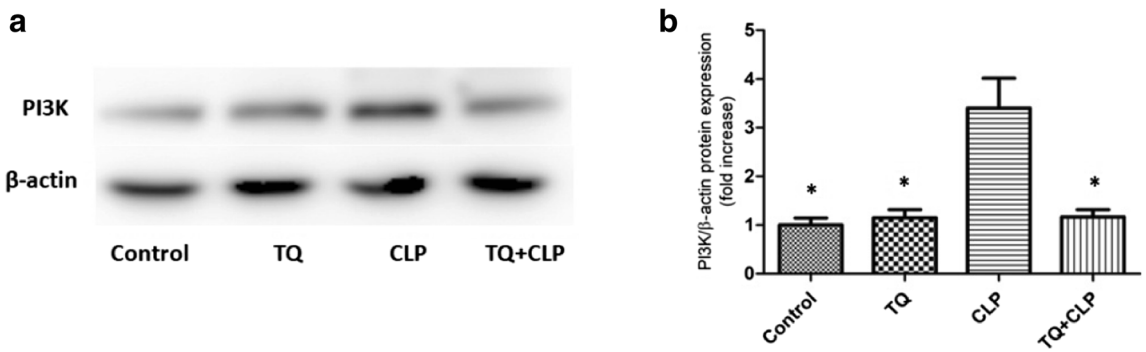

Fig. 5. PI3K levels in the cardiac tissues of the four groups of BALB/c mice after various treatments. **a** Immunoblotting to detect the PI3K level in the cardiac tissues. **b** Bar graph depicts the quantification of PI3K expression level. Data are shown as mean ± SEM; $n = 3–4$ in each group. *$P < 0.05$ *vs.* the CLP group.

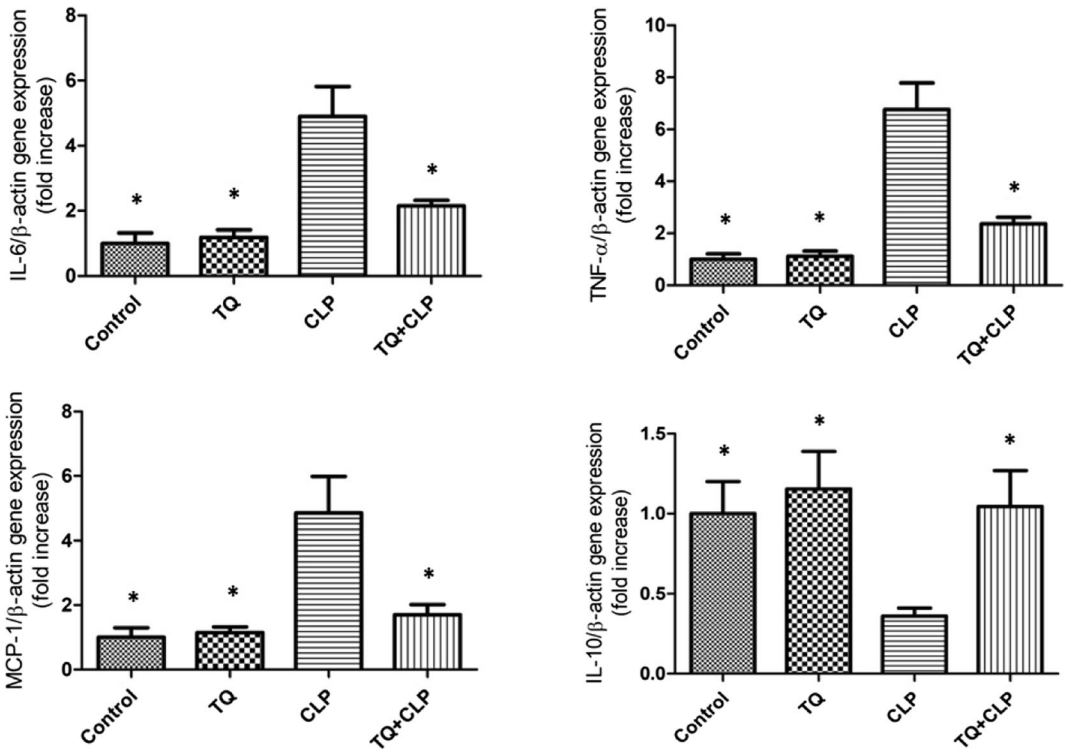

Fig. 6. Expression of pro-inflammatory genes in the cardiac tissues from the BALB/c mice of the four groups after treatment. Relative mRNA expression of IL-6, TNF-α, MCP-1, and IL-10 in the cardiac tissues of the four groups after treatment. Data are given as mean ± SEM; $n = 6$ in each group. *$P < 0.05$ *vs.* the CLP group.

sepsis [29]. Thus, NLRP3 could be a promising molecular target for sepsis treatment. Many studies have shown that NLRP3 recruits caspase-1, leading to the activation of caspase-1, maturation and secretion of IL-1β and IL-18, and initiation of pyroptosis [30–33]. Our results showed that TQ + CLP group had markedly reduced NLRP3, caspase-1, IL-1β, and IL-18 expressions in the cardiac tissues compared to the CLP group. These results indicate that TQ downregulated pyroptosis in the CLP group mice.

Previous studies suggested that the PI3K pathway is closely associated with autophagy and pyroptosis. Zhang et al. suggested that the PI3K/protein kinase B (Akt)/mammalian target of the rapamycin signaling pathway is involved in Schisandrin B-induced autophagy in AML-12 and RAW 264.7 cells [34–36]. Our study showed that the TQ + CLP group exhibited significantly suppressed PI3K levels compared to the CLP group. Thus, it is speculated that TQ regulates autophagy and pyroptosis *via* the PI3K pathway.

Pro-inflammatory genes (TNF-α, IL-6, and MCP-1) are reportedly expressed at high levels and contribute to cardiac damage in sepsis [37, 38]. PI3K pathway also is closely associated with inflammatory cytokines [39]. The present study showed that TNF-α, IL-6, and MCP-1 gene expressions were reduced in the TQ + CLP group compared to the CLP group.

Our study established that TQ contributes to the mitigation of sepsis-induced cardiac damage *via* autophagy, pyroptosis, and pro-inflammatory cytokine expression. These findings provide new insight into the role of TQ in sepsis-induced cardiac damage and raise the possibility of a novel therapeutic intervention to prevent the progression of cardiovascular diseases.

AUTHORS' CONTRIBUTIONS

Zuowei Pei designed this study; Hongyang Liu, Guang Yang, and Yue Zhao helped in performing experiments; Zuowei Pei and Yan Sun analyzed data and interpreted the results of experiments; Lipeng Guo and Ying Zhang prepared figures; Hongyang Liu drafted the manuscript. All authors read and approved the final manuscript.

FUNDING INFORMATION

This work was finally supported by the Posterdoctor Foundation of Liaoning Province, China (No. 194008).

COMPLIANCE WITH ETHICAL STANDARDS

Conflicts of Interest. The authors declare that they have no conflict of interest.

REFERENCES

1. Gaieski, D.F., J.M. Edwards, M.J. Kallan, and B.G. Carr. 2013. Benchmarking the incidence and mortality of severe sepsis in the United States. *Critical Care Medicine* 41: 1167–1174.
2. Kaukonen, K.M., M. Bailey, D. Pilcher, D.J. Cooper, and R. Bellomo. 2015. Systemic inflammatory response syndrome criteria in defining severe sepsis. *The New England Journal of Medicine* 372: 1629–1638.
3. Gao, Y.L., M.M. Yu, S.T. Shou, Y. Yao, Y.C. Liu, L.J. Wang, B. Lu, and Y.F. Chai. 2016. Tuftsin prevents the negative immunoregulation of neuropilin-1highCD4+CD25+regulatory T cells and improves survival rate in septic mice. *Oncotarget* 7: 81791–81805.
4. Cimolai, M.C., S. Alvarez, C. Bode, and H. Bugger. 2015. Mitochondrial mechanisms in septic cardiomyopathy. *International Journal of Molecular Sciences* 16: 17763–17778.
5. Rudiger, A., and M. Singer. 2007. Mechanisms of sepsis-induced cardiac dysfunction. *Critical Care Medicine* 35: 1599–1608.
6. Zanotti-Cavazzoni, S.L., and S.M. Hollenberg. 2009. Cardiac dysfunction in severe sepsis and septic shock. *Current Opinion in Critical Care* 15: 392–397.
7. Levine, B., and G. Kroemer. 2008. Autophagy in the pathogenesis of disease. *Cell* 132: 27–42.
8. Mizushima, N., B. Levine, A.M. Cuervo, and D.J. Klionsky. 2008. Autophagy fights disease through cellular self-digestion. *Nature* 451: 1069–1075.
9. Pu, Q., C. Gan, R. Li, Y. Li, S. Tan, X. Li, Y. Wei, L. Lan, X. Deng, H. Liang, F. Ma, and M. Wu. 2017. Atg7 deficiency intensifies inflammasome activation and pyroptosis in Pseudomonas sepsis. *Journal of Immunology* 198: 3205–3213.
10. Pfalzgraff, A., L. Heinbockel, Q. Su, K. Brandenburg, and G. Weindl. 2017. Synthetic anti-endotoxin peptides inhibit cytoplasmic LPS-mediated responses. *Biochemical Pharmacology* 140: 64–72.
11. Aglietti, R.A., and E.C. Dueber. 2017. Recent insights into the molecular mechanisms underlying pyroptosis and gasdermin family functions. *Trends in Immunology* 38: 261–271.
12. Esquerdo, K.F., N.K. Sharma, M.K.C. Brunialti, G.L. Baggio-Zappia, M. Assunção, L.C.P. Azevedo, A.T. Bafi, and R. Salomao. 2017. Inflammasome gene profile is modulated in septic patients, with a greater magnitude in non-survivors. *Clinical and Experimental Immunology* 189: 232–240.
13. Gali-Muhtasib, H., A. Roessner, and R. Schneider-Stock. 2006. Thymoquinone: A promising anti-cancer drug from natural sources. *The International Journal of Biochemistry & Cell Biology* 8: 1249–1253.
14. Xu, J., L. Zhu, H. Liu, M. Li, Y. Liu, F. Yang, and Z. Pei. 2018. Thymoquinone reduces cardiac damage caused by hypercholesterolemia in apolipoprotein E-deficient mice. *Lipids in Health and Disease* 17: 173.
15. Pei, Zuowei, Jiahui Hu, Qianru Bai, Baiting Liu, Cheng Dong, Hainiang Liu, Rongmei Na, and Yu. Qin. 2018. Thymoquinone protects against cardiac damage from doxorubicin-induced heart failure in Sprague-Dawley rats. *RSC Advances* 8: 14633–14639.
16. Rittirsch, D., M.S. Huber-Laang, M.A. Flierl, and P.A. Ward. 2009. Immunodesign of experimental sepsis by cecal ligation and puncture. *Nature Protocols* 4: 31–36.
17. Chu, M., Y. Gao, Y. Zhang, B. Zhou, B. Wu, J. Yao, and D. Xu. 2015. The role of speckle tracking echocardiography in assessment of lipopolysaccharide-induced myocardial dysfunction in mice. *Journal of Thoracic Disease* 12: 2253–2261.
18. Flierl, M.A., D. Rittirsch, M.S. Huber-Lang, J.V. Sarma, and P.A. Ward. 2008. Molecular events in the cardiomyopathy of sepsis. *Molecular Medicine* 14: 327–336.
19. Hsieh, C.H., P.Y. Pai, H.W. Hsueh, S.S. Yuan, and Y.C. Hsieh. 2011. Complete induction of autophagy is essential for cardioprotection in sepsis. *Annals of Surgery* 253: 1190–1200.
20. Zhang, J., P. Zhao, N. Quan, L. Wang, X. Chen, C. Cates, T. Rousselle, and J. Li. 2017. The endotoxemia cardiac dysfunction is attenuated by AMPK/mTOR signaling pathway regulating autophagy. *Biochemical and Biophysical Research Communications* 492: 520–527.
21. Zilinyi, R., A. Czompa, A. Czegledi, A. Gajtko, D. Pituk, I. Lekli, and A. Tosaki. 2018. The Cardioprotective effect of metformin in doxorubicin-induced cardiotoxicity: The role of autophagy. *Molecules* 23: E1184.
22. Zheng, Y., S. Gu, X. Li, J. Tan, S. Liu, Y. Jiang, C. Zhang, L. Gao, and H.T. Yang. 2017. Berbamine postconditioning protects the heart from ischemia/reperfusion injury through modulation of autophagy. *Cell Death & Disease* 8: e2577.
23. Su, Y., Y. Qu, F. Zhao, H. Li, D. Mu, and X. Li. 2015. Regulation of autophagy by the nuclear factor κB signaling pathway in the hippocampus of rats with sepsis. *Journal of Neuroinflammation* 12: 116.
24. Aziz, M., A. Jacob, and P. Wang. 2014. Revisiting caspases in sepsis. *Cell Death & Disease* 5: e1526.
25. Vande Walle, L., and M. Lamkanfi. 2016. Pyroptosis. *Current Biology* 26: R568–R572.
26. Yang, Y., G. Jiang, P. Zhang, and J. Fan. 2015. Programmed cell death and its role in inflammation. *Military Medical Research* 2: 12.
27. Man, S.M., R. Karki, and T.D. Kanneganti. 2017. Molecular mechanisms and functions of pyroptosis, inflammatory caspases and inflammasomes in infectious diseases. *Immunological Reviews* 277: 61–75.
28. Lee, S., K. Nakahira, J. Dalli, I.I. Siempos, P.C. Norris, R.A. Colas, J.S. Moon, M. Shinohara, S. Hisata, J.A. Howrylak, G.Y. Suh, S.W. Ryter, C.N. Serhan, and A.M.K. Choi. 2017. NLRP3 Inflammasome deficiency protects against microbial sepsis via increased Lipoxin B4 synthesis. *American Journal of Respiratory and Critical Care Medicine* 196: 713–726.
29. Wu, Y., J. Ren, B. Zhou, C. Ding, J. Chen, G. Wang, G. Gu, X. Wu, S. Liu, D. Hu, and J. Li. 2015. Gene silencing of non-obese diabetic receptor family (NLRP3) protects against the sepsis-induced hyperbile acidaemia in a rat model. *Clinical and Experimental Immunology* 179: 277–293.

30. Bordon, Y. 2012. Mucosal immunology: Inflammasomes induce sepsis following community breakdown. *Nature Reviews, Immunology* 12: 400–401.
31. Gonçalves, A.C., L.S. Ferreira, F.A. Manente, C.M.Q.G. de Faria, M.C. Polesi, C.R. de Andrade, D.S. Zamboni, and I.Z. Carlos. 2017. The NLRP3 inflammasome contributes to host protection during Sporothrix schenckii infection. *Immunology* 151: 154–166.
32. Borges, P.V., K.H. Moret, N.M. Raghavendra, T.E. Maramaldo Costa, A.P. Monteiro, A.B. Carneiro, P. Pacheco, J.R. Temerozo, D.C. Bou-Habib, M. das Graças Henriques, and C. Penido. 2017. Protective effect of gedunin on TLR-mediated inflammation by modulation of inflammasome activation and cytokine production: Evidence of a multitarget compound. *Pharmacological Research* 115: 65–77.
33. Liston, A., and S.L. Masters. 2017. Homeostasis-altering molecular processes as mechanisms of inflammasome activation. *Nature Reviews Immunology* 17: 208–214.
34. Zhang, Y., Z.W. Zhou, H. Jin, C. Hu, Z.X. He, Z.L. Yu, K.M. Ko, T. Yang, X. Zhang, S.Y. Pan, and S.F. Zhou. 2015. Schisandrin B inhibits cell growth and induces cellular apoptosis and autophagy in mouse hepatocytes and macrophages: Implications for its hepatotoxicity. *Drug Design, Development and Therapy* 9: 2001–2027.
35. Xu, S., L. Wu, Q. Zhang, J. Feng, S. Li, J. Li, T. Liu, W. Mo, W. Wang, X. Lu, Q. Yu, K. Chen, Y. Xia, J. Lu, L. Xu, Y. Zhou, X. Fan, and C. Guo. 2017. Pretreatment with propylene glycol alginate sodium sulfate ameliorated concanavalin A-induced liver injury by regulating the PI3K/Akt pathway in mice. *Life Sciences* 185: 103–113.
36. Li, Z., F. Zhao, Y. Cao, J. Zhang, P. Shi, X. Sun, F. Zhang, and L. Tong. 2018. DHA attenuates hepatic ischemia reperfusion injury by inhibiting pyroptosis and activating PI3K/Akt pathway. *European Journal of Pharmacology* 835: 1–10.
37. Kakihara, Y., T. Ito, M. Nakahara, K. Yamaguchi, and T. Yasuda. 2016. Sepsis-induced myocardial dysfunction: Pathophysiology and treatment. *Journal of Intensive Care* 4: 22.
38. Pfeiffer, D., E. Roßmanith, I. Lang, and D. Falkenhagen. 2017. miR-146a, miR-146b, and miR-155 increase expression of IL-6 and IL-8 and support HSP10 in an in vitro sepsis model. *PLoS One* 29: e0179850.
39. Liu, Y., R. Liao, Z. Qiang, and C. Zhang. 2017. Pro-inflammatory cytokine-driven PI3K/Akt/Sp1 signalling and H2S production facilitates the pathogenesis of severe acute pancreatitis. *Bioscience Reports* 37 (2): BSR20160483. https://doi.org/10.1042/BSR20160483.